Available online at www.sciencedirect.com

ScienceDirect

www.elsevier.com/locate/matchar

Accurate modeling and reconstruction of three-dimensional percolating filamentary microstructures from two-dimensional micrographs via dilation-erosion method

En-Yu Guo[a,b], Nikhilesh Chawla[b], Tao Jing[a], Salvatore Torquato[c,d,e,f], Yang Jiao[b,*]

[a]Key Laboratory for Advanced Materials Processing Technology, School of Materials Science and Engineering, Tsinghua University, Beijing 100084, China
[b]Materials Science and Engineering, School for Engineering of Matter, Transport, and Energy, Arizona State University, Tempe, AZ 85287, USA
[c]Department of Chemistry, Princeton University, Princeton, NJ 08544, USA
[d]Department of Physics, Princeton University, Princeton, NJ 08544, USA
[e]Princeton Institute for the Science and Technology of Materials, Princeton University, Princeton, NJ 08544, USA
[f]Program in Applied and Computational Mathematics, Princeton University, Princeton, NJ 08544, USA

ARTICLE DATA

Article history:
Received 30 October 2013
Received in revised form
21 December 2013
Accepted 23 December 2013

Keywords:
3D microstructure reconstruction
Dilation–erosion
Topologically complex microstructure
Austenitic–ferritic stainless steel

ABSTRACT

Heterogeneous materials are ubiquitous in nature and synthetic situations and have a wide range of important engineering applications. Accurate modeling and reconstructing three-dimensional (3D) microstructure of topologically complex materials from limited morphological information such as a two-dimensional (2D) micrograph is crucial to the assessment and prediction of effective material properties and performance under extreme conditions. Here, we extend a recently developed dilation–erosion method and employ the Yeong–Torquato stochastic reconstruction procedure to model and generate 3D austenitic–ferritic cast duplex stainless steel microstructure containing percolating filamentary ferrite phase from 2D optical micrographs of the material sample. Specifically, the ferrite phase is dilated to produce a modified target 2D microstructure and the resulting 3D reconstruction is eroded to recover the percolating ferrite filaments. The dilation–erosion reconstruction is compared with the actual 3D microstructure, obtained from serial sectioning (polishing), as well as the standard stochastic reconstructions incorporating topological connectedness information. The fact that the former can achieve the same level of accuracy as the latter suggests that the dilation–erosion procedure is tantamount to incorporating appreciably more topological and geometrical information into the reconstruction while being much more computationally efficient.

1. Introduction

Heterogeneous materials such as composites, alloys, granular materials and porous media abound in nature and in engineering applications. Applications of heterogeneous materials in civil, industrial and aerospace engineering require accurate assessments and predictions of the effective material properties and their performance under extreme conditions, which in turn rely on the accurate knowledge of the complex material microstructures. In the past few decades, a quantitative under-

* *Corresponding author*. Tel.: +1 4809654560; fax: +1 4809659973.
E-mail address: yang.jiao.2@asu.edu (Y. Jiao).

1044-5803/$ – see front matter © 2013 Elsevier Inc. All rights reserved.
http://dx.doi.org/10.1016/j.matchar.2013.12.011

standing of the microstructure and structure–property relation of heterogeneous materials has begun to emerge, mainly due to the development of advanced experimental and computational material microstructure characterization techniques [1–3]. Specifically, advanced imaging techniques such as X-ray tomographic microscopy [4–6], which eliminates destructive cross-sectioning and allows for superior resolution and image quality with minimal sample preparation [7,8], have been widely used to obtain high-resolution three-dimensional (3D) microstructure for a wide range of heterogeneous materials, including Sn-rich alloys [9], powder metallurgy steels [10], metal matrix composites [11–15], and lightweight alloys [16–20]. On the theory side, a zoology of statistical microstructure descriptors has been presented and derived from rigorous structure–property analysis [1,2]. For example, the canonical n-point correlation function H_n [2], the integrals of which are involved in various rigorous bounds [21] and contrast expansions [22,23] of effective material properties, gives the probability of finding a specific n-point configuration in the phase of interest. A variety of non-canonical descriptors providing topological connectedness information [24–26] and interface information [27] have also been devised and applied to study a wide spectrum of materials.

Despite of rapid advances of non-destructive 3D imaging techniques, there are still material systems for which only 2D images are available. For example, in certain alloys the contrast between the absorption rates of probing rays associated with different phases is too weak to resolve the individual phases. In such situations, usually the only available structural data obtained from non-destructive means are 2D electron micrographs or optical images of the sample surfaces, which does not contain topological connectedness information of the material phases [2]. Although serial sectioning can be employed to obtain full 3D microstructure, this procedure is very tedious and will completely destroy the material sample. Therefore, it is highly desirable to render realistic virtual 3D microstructures that faithfully present the limited morphological information contained in the available 2D data sets, albeit with 3D experimental verification.

Over the past two decades, a variety of microstructure reconstruction methods from limited structural information have been developed, including the Gaussian random field method [28], stochastic reconstruction procedure [29,30], phase recovery method [31], multi-point reconstruction method [32], and raster-path method [33]. The Gaussian random field method [28] was originally devised to reconstruct realizations of statistically homogeneous and isotropic random media from the associated two-point correlation functions. Specifically, a field-field correlation function is constructed based on the given two-point correlation function S_2 (see definition in Section. 2). A Gaussian random field is then generated using the field-field correlation function, whose level-cut results in a binary microstructure associated the target two-point function. Although a wide class of microstructures can be obtained using this method, the morphological information used for reconstruction is limited to the two-point correlation functions [28]. The phase recovery method enables one to take into account the full vector information contained in the two-point statistics associated with the material, and thus allows the reconstructions of complex anisotropic microstructure and polycrystalline materials [31]. This method proceeds by iteratively solving for the phase information that is lost when representing the microstructure using the vector two-point correlation functions. Once such phase information is successfully recovered, the microstructure can be directly obtained via fast Fourier transform.

The multi-point reconstruction method was originally developed for the reconstruction of porous geomaterials from 2D images [32]. Instead of using two-point statistics associated with the entire 2D microstructure, this method incorporates all n-point statistics within a smaller window containing a portion of the microstructure. The window size is determined by the correlation length of the material. A sequential addition method is then employed to put down voxels in an initially empty reconstruction domain based on the n-point statistics to generate a 3D microstructure. Although more accurate reconstructions can be obtained due to the additional morphological information contained in the multi-point statistics, it is difficult to efficiently store, represent and retrieve the n-point statistics even for a very small window. Recently, a raster-path method is devised which allows one to employ the multi-point statistics in a much more efficient way [33]. Specifically, instead of extracting the statistics from the 2D microstructure, a cross-correlation function is introduced to directly compare a reconstructed portion of the material to the target 2D image. Only the reconstructed portions that sufficiently well match a portion in the target microstructure will be accepted and inserted into an initially empty reconstruction domain along a 1D raster path [33].

The stochastic reconstruction procedure [29,30] (also referred to as Yeong–Torquato procedure in literature) enables one to incorporate an arbitrary number of correlation functions of any types into the reconstructions. Specifically, a random initial microstructure is evolved using simulated annealing procedure such that the set of correlation functions sampled from the reconstructed microstructure match the corresponding set of target statistics up to a prescribed small tolerance (see Section. 3 for algorithmic details). This reconstruction procedure is very flexible and versatile, however, due to its stochastic nature a large number of intermediate microstructures need to be generated and analyzed, which makes it computationally intensive. Several different implementations of the Y–T procedure have been devised to improve efficiency [34–36], preserve isotropy [37–39] or handle anisotropic materials [40]. In particular, a dilation–erosion (DE) method based on the Y–T procedure has recently been proposed by Zachary and Torquato to improve the accuracy of the reconstructions of topologically complex microstructures [41]. The DE method (discussed in detail in Section. 3) has been applied to successfully reconstruct 2D model microstructures including multiply connected "donut" media and random distributions of micro-cracks [41].

In this paper, we will extend the dilation–erosion procedure devised by Zachary and Torquato [41] for 2D random textures to accurately model and reconstruct 3D filamentary microstructures from limited morphological information (e.g., certain spatial correlation functions associated with the filamentary phase) available in 2D images of the material. We will focus on austenitic–ferritic cast duplex stainless steels for which the 2D optical micrographs of the sample surfaces (see Fig. 1) will be used as the input for the reconstruction. As shown in Fig. 1, the filamentary structures correspond to the ferrite phase which percolates in three dimensions. Such percolating filamentary

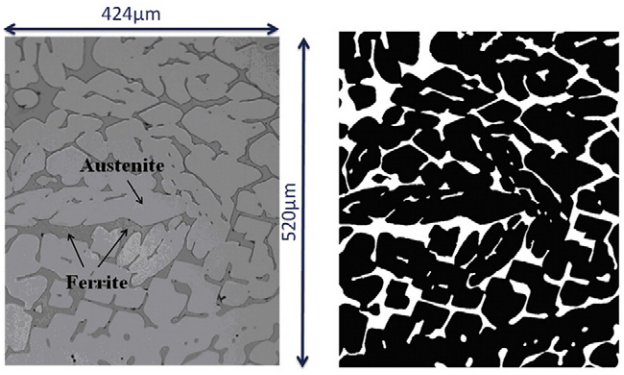

Fig. 1 – Left panel: Optical micrograph of the surface of an austenitic–ferritic cast duplex stainless steel. Right panel: The segmented binary image associated with the optical micrograph.

structures abound in a wide spectrum of material systems including grain-boundary networks, binary composites, and geological structures, to name but a few. And a variety of quantitative morphological descriptors for such structures have been devised [42–45]. A thin 3D microstructure reconstruction will be obtained via serial sectioning in order to ascertain the accuracy of the stochastic reconstructions. The two-point correlation function S_2 sampled from 2D micrographs will be used in both the standard reconstruction (without dilation–erosion of the phases) and the dilation–erosion reconstruction, in which the filamentary phase is dilated when sampling S_2 and eroded in the 3D reconstructions. For the austenitic–ferritic cast duplex stainless steel under consideration, which is statistically homogeneous and isotropic, S_2 sampled from 2D micrographs is representative of that obtained from full 3D material [2]. In addition, the two-point cluster function C_2 of the un-dilated ferrite phase, which contains additional topological information of the microstructure [26,36] (see definition below), will be directly obtained from the 3D experimentally reconstructed obtained microstructure and incorporated into the standard reconstructions without dilation/erosion (unlike in Ref. [41]). We show that the dilation–erosion method can lead to much more accurate reconstructions than the standard method using S_2 obtained from un-dilated 2D micrographs, which underestimates the linear extent and connectivity of the filamentary ferrite phase. Our results indicate that the dilation–erosion process considered in this work is tantamount to the use of the three dimensional cluster function C_2, and thus can better capture the topological connectedness information of the filamentary structures. The important point to note, since only S_2 of the dilated phase is incorporated into the reconstruction procedure, the computational cost associated with the DE reconstruction is significantly lower than that of the reconstruction incorporating C_2, which involves keeping track of the complex clusters during the evolution of the microstructure. This suggests that the dilation–erosion method could provide an efficient tool for the modeling and characterization of complex filamentary microstructures.

The rest of the paper is organized as follows: In Section. 2, we provide definitions of the statistical descriptors used to characterize the filamentary microstructures. In Section. 3, we describe the stochastic reconstruction procedure and the dilation–erosion method in detail. In Section. 4, we present and analyze the reconstruction results. In Section. 5, we make concluding remarks.

2. Statistical Microstructure Descriptors

2.1. Two-Point Correlation Function

In general, the microstructure of a heterogeneous material can be uniquely determined by specifying the indicator functions associated with all of the individual phases of the material [2], i.e.,

$$I^{(i)}(\mathbf{x}) = \begin{cases} 1 & \mathbf{x} \text{ in phase } i \\ 0 & \text{otherwise} \end{cases} \tag{1}$$

where i = 1, …, q and q is the total number of phases. The volume fraction of phase i is then given by

$$\varphi_i = < I^{(i)}(\mathbf{x}) > \tag{2}$$

where <> denotes the ensemble average over many independent material samples or volume average over a single large sample if it is spatially "ergodic" [2]. The two-point correlation function $S_2^{(ij)}(\mathbf{x}_1,\mathbf{x}_2)$ associated with phases i and j is defined as

$$S_2^{(ij)}(\mathbf{x}_1,\mathbf{x}_2) = < I^{(i)}(\mathbf{x}_1) I^{(j)}(\mathbf{x}_2) > \tag{3}$$

which also gives the probability that two randomly selected points x_1 and x_2 fall into phase i and j respectively (see Fig. 2A). For a material with q distinct phases, there are totally q^2 different S_2. However, it has been shown that only $q - 1$ of them are independent [2,31] and the remaining $q^*(q - 1) + 1$ functions can be explicitly expressed in terms of the q independent ones. In our case, $q = 2$ (filamentary structures in a matrix) and thus, we can only consider the two-point correlation function associated with the filamentary structures. In the ensuing discussion, we will focus the correlation function for the phase of interest and drop the superscript in the function for convenience.

For a statistically homogeneous and isotropic material such as the stainless steel considered here, there are no preferred center and direction in the microstructure. Therefore, the associated S_2 for the phase of interest depends only on the relative distance between the two points [2], i.e.,

$$S_2(\mathbf{x}_1,\mathbf{x}_2) = S_2(|\mathbf{x}_2 - \mathbf{x}_1|) = S_2(r) \tag{4}$$

where $r = |r| = |x_2 - x_1|$. At $r = 0$ the quantity $S_2(0)$ gives the probability that a randomly selected point falls into the phase of interest, i.e., the volume fraction of the associated phase $S_2(r = 0) = \varphi$. At large r values, the probabilities of finding the two points in the phases of interest are independent of one another, leading to $S_2(r \to \infty) = \varphi^2$. Importantly, it has been shown that for statistically homogeneous and isotropic microstructures, the associated S_2 can be obtained from the low-dimensional cuts of the microstructure (e.g., 2D slices of a 3D material) [2]. In other words, the S_2 of 2D slices contains morphological information that is representative of the original

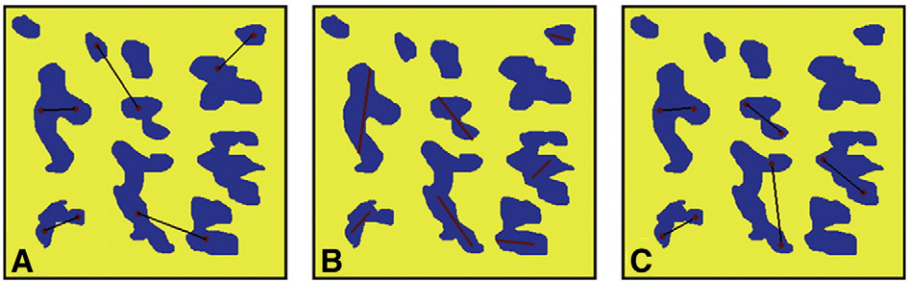

Fig. 2 – Schematic illustrations of the events contributing to different correlation functions. The two-point correlation function S_2 gives the probably of finding two points in the phases of interest. In (A), we show events that contribute to S_2 associated with the blue phase. The lineal-path function $L(r)$ gives the probability that a randomly chosen line segment of length r entirely falls into the phase of interest. In (B), we show events that contribute to L associated with the blue phase. The two-point cluster function $C_2(r)$ gives the probability of finding two points separated by r in the same cluster of the phase of interest. In (C), we show events that contribute to C_2 associated with the blue phase.

3D microstructure. This makes it a very useful quantity for reconstructing 3D microstructures from 2D images.

We note that the general n-point correlation function S_n which gives the probability of finding a particular n-point configuration in specific phases can be defined in a similar manner as S_2 [c.f. Eq. (2)], i.e.,

$$S_n(\mathbf{x}_1, \mathbf{x}_2, \ldots, \mathbf{x}_n) = < I(\mathbf{x}_1) I(\mathbf{x}_2) \cdots I(\mathbf{x}_n) > \quad (5)$$

It has been shown that the effective properties of a heterogeneous material can be explicitly expressed as series expansions involving certain integrals of S_n. Interested readers are referred to Ref. [2] for detailed discussions of S_n and their properties.

2.2. Lineal-Path Function

The lineal-path function $L^{(i)}(r)$ gives probability that a randomly selected line segment of length $r = |r|$ along the direction of vector r entirely falls into phase i (see Fig. 2B) [2,24]. At $r = 0$, $L^{(i)}(0)$ reduces to the probability of finding a point in phase i and thus, $L^{(i)}(0) = \varphi_i$. In materials that do not contain system-spanning clusters, the chances of finding a line segment with very large length entirely falling into any phases are vanishingly small. Accordingly, for large r values $L^{(i)}$ decays to zero rapidly in such materials, i.e., $L^{(i)}(r \to \infty) = 0$. The lineal-path function contains partial topological connectedness information of the material's phases, i.e., that along a lineal-path. Generally, the lineal-path function underestimates the degree of clustering in the system (e.g., two points belonging to the same cluster but not along a specific lineal path will not contribute to $L^{(i)}$).

2.3. Two-Point Cluster Function

The two-point cluster correlation function $C_2^{(i)}(\mathbf{x}_1,\mathbf{x}_2)$ gives the probability that two randomly selected points x_1 and x_2 fall into the same cluster of phase i (see Fig. 2C) [2,26]. For statistically homogeneous and isotropic materials, C_2 for the phase of interest depends only on the relative distance between the two points, i.e., $C_2(\mathbf{x}_1,\mathbf{x}_2) = C_2(|\mathbf{x}_1 - \mathbf{x}_2|) = C_2(r)$. In contrast to the lineal-path function, C_2 contains complete clustering information of the phases, which has been shown to have dramatic effects on the material's physical properties [2]. Moreover, unlike S_2 and L, the cluster functions generally cannot be obtained from lower-dimensional cuts (e.g., 2D slices) of a 3D microstructure, which may not contain correct connectedness information of the actual 3D system.

It has been shown that C_2 is related to S_2 via the following equation [26]

$$S_2(r) = C_2(r) + D_2(r) \quad (6)$$

where $D_2(r)$ measures the probability that two points separated by r fall into different clusters of the phase of interest. In other words, C_2 is the connectedness contribution to the standard two-point correlation function S_2. For microstructures with well-defined inclusion, C_2 (r) of the inclusions is a short-ranged function that rapidly decays to zero as r approaches the largest linear size of the inclusions. We note that although C_2 is a "two-point" quantity, it has been shown to embody higher-order structural information which makes it a highly sensitive statistical descriptor over and above S_2 [36,41].

3. Stochastic Reconstruction Procedures

3.1. Yeong–Torquato Reconstruction Procedure

We use the Yeong–Torquato (YT) reconstruction procedure [29,30] to generate virtual 3D microstructures from a specific set of correlation functions discussed in the previous Section. 2. As discussed in Section. 1, there are many other different microstructure reconstruction procedures, such as the Gaussian random field method [28], phase recovery method [31], multi-point reconstruction method [32] and the recently developed raster path method [33]. Importantly, the YT procedure is the most flexible and versatile one that enables us to incorporate an arbitrary number of correlation functions of any type.

In the YT procedure, the reconstruction problem is formulated as an "energy" minimization problem, with the energy functional E defined as follows

$$E = \sum_{\alpha} \sum_{r} \left[f^{\alpha}(r) - \hat{f}^{\alpha}(r) \right]^2 \quad (7)$$

where $\hat{f}^{\alpha}(r)$ is a target correlation function of type α and $f^{\alpha}(r)$ is the corresponding function associated with an intermediate microstructure. In the case that the set of target functions only includes the standard two-point correlation function, the "energy" formulation of the reconstruction problem has been successfully solved using other schemes such as the gradient-based method [46] and iterative procedures [31]. The simulated annealing method [47] is employed here to solve the aforementioned minimization problem. Specifically, starting from an initial microstructure (i.e., *old* microstructure) which contains a fixed number of voxels for each phase consistent with the volume fraction of that phase, two randomly selected voxels associated with different phases are exchanged to generate a *new* microstructure. Relevant correlation functions are sampled from the new microstructure and the associated energy is evaluated, which determines whether the new microstructure should be accepted or not via the probability:

$$p_{acc}(old \rightarrow new) = \min\left\{1, \quad \exp\left(\frac{E_{old}-E_{new}}{T}\right)\right\} \tag{8}$$

where T is a virtual temperature that is chosen to be initially high and slowly decreases according to a cooling schedule [29,30]. The above process is repeated until E is smaller than a prescribed tolerance, which we choose to be 10^{-10} here. Generally, several hundred thousand trials need to be made to achieve such a small tolerance. Therefore, efficient sampling methods [36–38] are used that enable one to rapidly obtain the prescribed correlation functions of a new microstructure by updating the corresponding functions associated with the old microstructure, instead of completely re-computing the functions.

3.2. Dilation–Erosion Method

For a topologically complex microstructure such as percolating thin filaments in a matrix, it is difficult to accurately capture the key structural features using a limited number of associated correlation functions [48,49]. Instead, we consider a modified microstructure that involves uniformly "dilating" or "eroding" a reference phase in the direction normal to the two-phase interface in the original microstructure [41]. Specifically, the dilation can be achieved by placing a virtual sphere of radius δ into the non-reference phase and determining the space available to the sphere as if the reference phase was impenetrable to the virtual sphere [1]. The space unavailable to the sphere is considered to be the dilated reference phase. The erosion process simply reverses this procedure such that the reference phase is allowed to be penetrated by a distance δ normal to the two-phase interface. In our implementations, we chose $\delta = 1$ pixel and the dilation (erosion) process simply corresponds to converting the pixels of the non-reference (reference) phase bordering the reference (non-reference) phase into the reference (non-reference) phase; see Fig. 3 for illustration. We will elaborate on this selection of δ in the discussion section.

To reconstruct a filamentary microstructure from 2D images, a dilation operation is first applied to the original 2D images. This leads to a modified 2D microstructure with thick "stripe-like" structures. The two-point correlation functions associated with the modified 2D microstructure are then computed and used as the input (i.e., target functions) for the Yeong–Torquato reconstruction procedure. As discussed in Section. 2.1, although the S_2's are sampled from 2D images, the morphological information contained in such correlation functions is representative of the 3D microstructure. After a 3D reconstruction is obtained, an erosion operation is applied to the 3D microstructure to recover the thin filaments. The degree of dilation (erosion) is determined by the parameter δ, which is the "thickness" of the dilated region. The choice of this parameter depends on the systems under consideration. A general rule is that the selected δ should be large enough to produce a percolated phase in the dilated microstructure such as the two-point correlation function S_2 of the dilated phase can lead to an accurate reconstruction.

4. Results

4.1. Experimental Results

The material studied in this work is a commercially available austenitic–ferritic cast duplex stainless steel (Z3CN20-09 M). The sample used to obtain the microstructures was machined from a centrifugally cast pipe which was heat treated at 1105 ± 10 °C for 4.5 h and then water-quenched. More microstructural information of the material can also be found in Ref. [50].

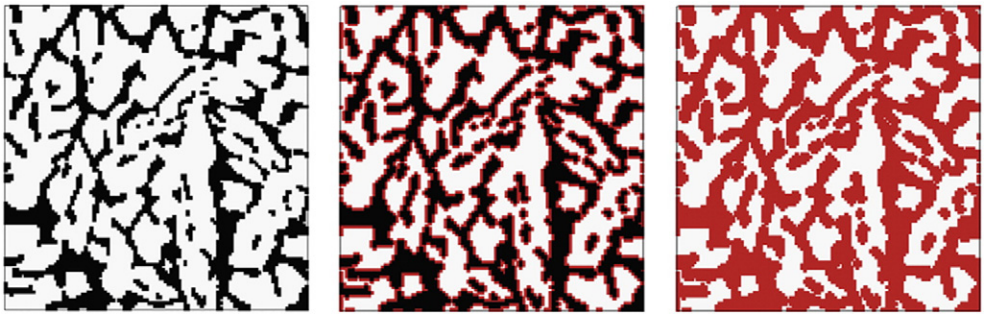

Fig. 3 – Schematic illustration of the dilation–erosion procedure. The leftmost panel shows an original filamentary microstructure. As shown in the middle panel, the reference (black) phase is uniformly dilated in the direction normal to the two-phase interface. The resulting modified microstructure after the dilation process is complete is shown in the rightmost panel. It can be seen that the dilation process maps the original filamentary structures into percolating stripe-like structures. The erosion process is just the inverse of the dilation procedure, which should lead to a better rendition of the original un-dilated system.

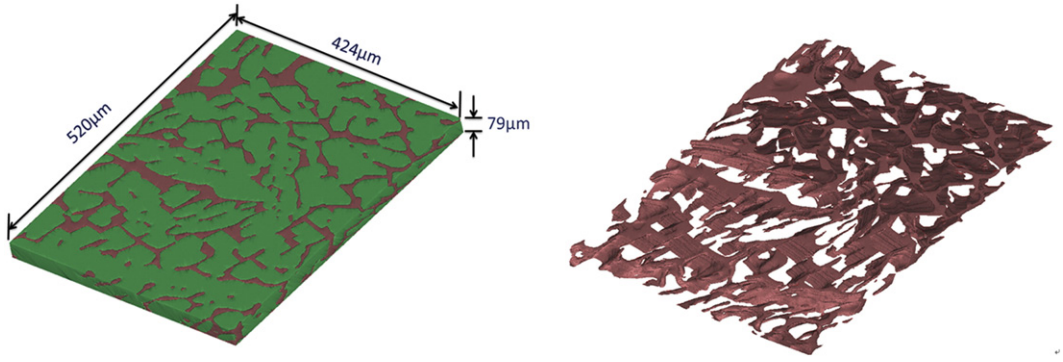

Fig. 4 – Left panel: Experimentally reconstructed microstructure of the cast duplex stainless steel showing the austenite matrix (in green) and ferrite phase (in red) obtained via the serial sectioning technique. Right panel: Extracted 3D ferrite phase morphology.

In order to acquire the 3D microstructure of the material, the serial-sectioning method [51] was utilized and the sample was polished using a semi-automatic polisher (MiniMet® 1000, Buehler company, Illinois, U.S). Initially, the sample was polished with 0.3 μm Al_2O_3 solution and then, followed by polishing with 0.05 μm colloidal silica solution to minimize the material removal rate and to restore a good surface quality. After each polishing cycle, the microstructure was revealed by etching using a solution of 25 ml HCl, 25 ml HNO_3 and 50 ml H_2O and the optical micrographs of the microstructure were acquired using an optical microscope (FS100, Mitutoyo, Japan). A removal material thickness of around 1.7 μm for each slice, which was measured to be much smaller than the microstructural phases of interest, was obtained and great effort was made to maintain the same removal rate for each slice. The micrographs were aligned using MATLAB software and then segmented into black and white images using a commercial image analysis software (Image J, Bethesda. MD). Finally, all the 2D segmented images were imported into a 3D visualization software for reconstruction and analysis (Mimics, Materiallise NV, Leuven, Belgium).

The experimentally reconstructed 3D microstructure composed of ferrite phase (red) in the austenite matrix (green) is shown in Fig. 4A. The extracted 3D ferrite phase morphology is shown in Fig. 4B, from which the connectivity of the phase can be clearly seen. The volume fraction of the ferrite phase is $\varphi = 0.26$. We employ the two-point correlation function S_2, the lineal-path function L and the two-point cluster function C_2 to quantitatively characterize the geometrical and topological features of the ferrite phase. Since only a thin 3D microstructure is available, the correlation functions are only sampled in 2D slices perpendicular to the short direction of the sample. However, the 3D connectedness information is properly taken into account to compute the cluster function C_2. Specifically, a pair of points may belong to apparently distinct clusters in the 2D slice, which are actually connected in 3D. Such point pairs will contribute to C_2. The computed correlation functions are shown in Fig. 5. It can be seen that the 3D C_2 is long-ranged, indicating high connectivity of the ferrite phase in three dimensions.

4.2. *Three-Dimensional Reconstructions*

Three-dimensional reconstructions are obtained using both the standard YT procedure and the dilation–erosion method. The microstructures obtained from the standard reconstruction using S_2 sampled from 2D slices without dilation–erosion, the reconstruction using the combination of S_2 and C_2 sampled from the actual 3D microstructure, as well as from the dilation–erosion reconstruction using S_2 sampled from 2D slices, are respectively shown in Fig. 6A,B, and C. The corresponding reconstructed correlation functions are respectively shown in Fig. 7A,B, and C.

It can be clearly seen from Figs. 6A and 7A that the standard S_2-alone reconstruction without dilation/erosion significantly underestimates the linear extent and connectivity of the ferrite filaments, although the reconstructed S_2 is virtually indistinguishable from the target S_2. This is because in general S_2 alone is not sufficient to uniquely determine a microstructure, i.e., there are an enormous number of distinct microstructures that are compatible with a specific S_2 [49]. At low volume fractions (i.e., $\varphi = 0.26$), the number of compatible microstructures containing short filaments and compact clusters is much larger than the number of compatible microstructures with percolating filaments. Due to the stochastic nature of YT procedure, the probability of finding a microstructure with disconnected cluster is thus much higher. On the other hand, the standard reconstruction incorporating both S_2 and C_2 leads to a significantly

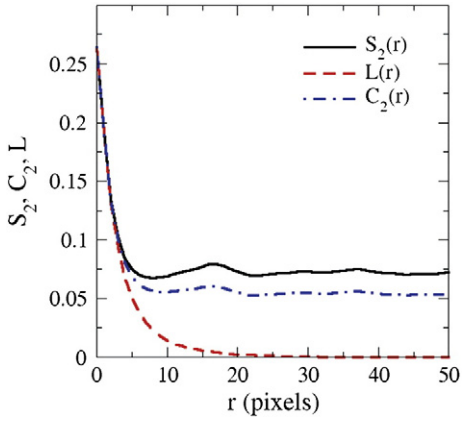

Fig. 5 – The correlation functions (defined in the text) associated with the percolating filamentary ferrite phase in the stainless steel microstructure. The unit of length is the side length of a pixel and 1 pixel = 3.8 μm.

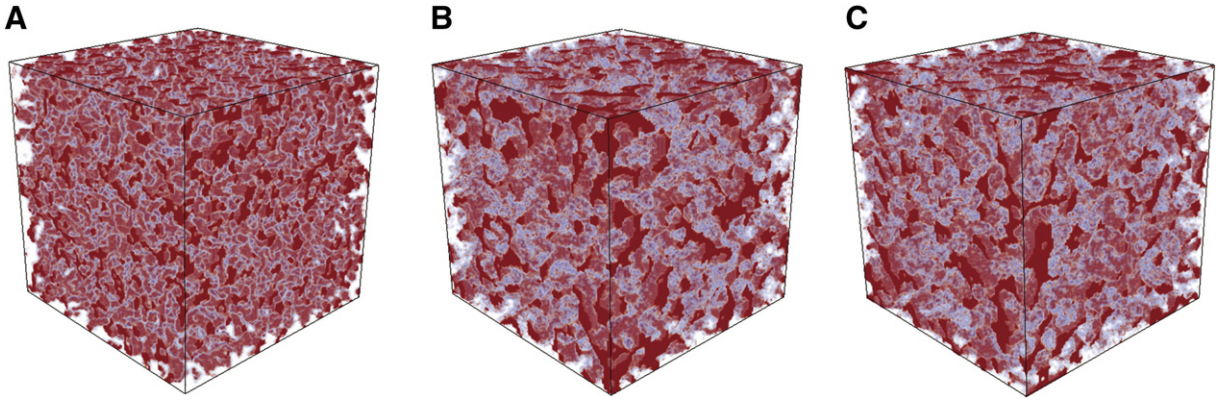

Fig. 6 – 3D microstructures obtained from the standard reconstruction using S_2 obtained from 2D micrographs without dilation/erosion (A), reconstruction incorporating S_2–C_2 sampled from 3D experimental obtained material microstructure (B), and the dilation–erosion reconstruction using S_2 of the dilated phases obtained from 2D micrographs (C). The linear size of the system is 400 μm. In (A), the linear sizes of the filaments are underestimated. The renditions of the filaments in (B) and (C) are significantly improved, due to the incorporation of additional topological connectedness information by directly using the cluster function C_2 (B) or the dilation–erosion procedure (C).

improved 3D microstructure, which can be seen both visually (see Fig. 6B) and from the comparison of the lineal-path functions associated with the reconstruction and the original microstructure (see Fig. 7B). The improved accuracy is due to the incorporation of additional topological connectedness information contained in the three dimensional C_2, which is crucial to capturing the salient features of percolating filamentary ferrite phase.

Fig. 6C shows the 3D microstructure reconstructed from S_2 alone using the dilation–erosion method. It can be seen both visually and from the comparison of the associated C_2 and L (see Fig. 7C) that the DE reconstruction also significantly improves up on the standard reconstruction using S_2 alone. Specifically, the cluster function C_2 associated with the DE reconstruction is long-ranged, indicating the high connectivity of the reconstructed filamentary ferrite phase. This is because by dilating the ferrite phase in the target 2D image, the phase volume fraction increases from 0.26 to 0.43, leading to percolating thick stripe-like structures. At $\varphi = 0.43$, the majority of the microstructures compatible with the given S_2 are composed of percolating stripe-like structures. Thus, the YT procedure has a high probability to find a microstructure with high connectivity. By applying an erosion operation on the initial reconstruction, the percolating filamentary ferrite phase is then recovered.

We note that although only S_2 from 2D slices is used, the 3D reconstruction obtained by the dilation–erosion method is comparable in accuracy to the reconstruction incorporating 3D C_2, which contains additional topological connectedness information. This implies that dilating or eroding the reference phase is tantamount to including connectedness information of the phase. However, since the reconstruction using C_2 requires one to keep track of the dynamics (e.g., forming and breaking) of the clusters for each intermediate microstructure [36], it is much more computationally intensive than the DE reconstruction, which only incorporates S_2; see Table 1 for the comparison of the CPU hours for different reconstructions.

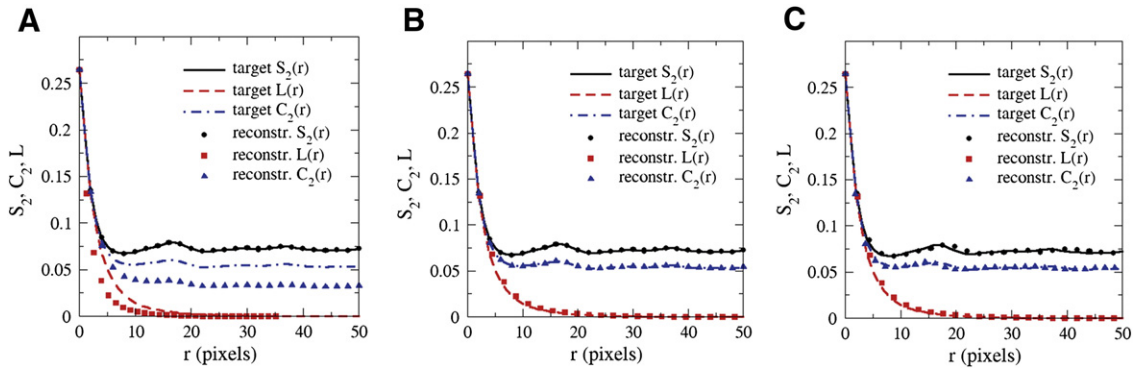

Fig. 7 – Comparison of the target and reconstructed correlation functions associated with the percolating filamentary ferrite phase. (A) Standard reconstruction using S_2 obtained from 2D micrographs without dilation/erosion (A), the reconstruction incorporating S_2–C_2 sampled from 3D experimental obtained material microstructure (B), and the dilation–erosion reconstruction using S_2 of the dilated phases obtained from 2D micrographs (C). The unit of length is the side length of a pixel and 1 pixel = 3.8 μm.

5. Summary and Discussion

We have extended the dilation–erosion method [41] to reconstruct topologically complex 3D microstructures from limited morphological information contained in 2D images. Specifically, we have focused on an austenitic–ferritic cast duplex stainless steel that contains percolating filamentary ferrite phase. The Yeong–Torquato reconstruction procedure was employed to generate 3D microstructures from the two-point correlation function S_2 sampled from 2D optical micrographs of the sample surface as well as from the two-point cluster function C_2 obtained from experimentally reconstructed 3D material microstructure. The key points are summarized in the following bulleted list:

- The standard reconstruction based on S_2 from 2D micrographs without dilation–erosion significantly underestimates the linear extent and connectivity of the ferrite phase, leading to isolated elongated clusters.
- On the other hand, the reconstruction incorporating three dimensional C_2, and thus additional topological connectedness information, reproduces the salient features of the percolating filamentary ferrite phase very well.
- The dilation–erosion reconstruction incorporating S_2 obtained from dilated 2D micrographs can lead to 3D microstructures with the level of accuracy comparable to the S_2-C_2 reconstruction using 3D structural information directly obtained from actual material microstructure. This suggests that dilating or eroding the reference phase is tantamount to including 3D connectedness information of the phase in the reconstruction.
- The computational cost of the DE reconstruction is significantly lower than the reconstruction incorporating the cluster function C_2.

A key parameter in the dilation–erosion reconstruction method is the dilation thickness δ which was chosen to be 1 pixel length in our implementation. As we mentioned in Section. 3.2, a general rule to determine the value of δ is that the selected value should lead to a percolating phase in the dilated microstructure. Too small δ values result in isolated phases which S_2 is insufficient to accurately characterize. On the other hand, too large δ values will produce significantly dilated phases that are difficult to recover during the erosion process. To quantify the effects of δ on the accuracy of the reconstruction, we reconstruct the filamentary stainless steel structure using different δ values, and compare the "errors" of the reconstructions, which are defined to be the squared difference between the reconstructed and target two-point cluster functions C_2; see Fig. 8. At $\delta = 0$, no dilation/erosion operations are applied during the reconstruction and thus, the procedure corresponds to the standard S_2 reconstruction, which is associated with an error E_0. For $\delta > 0$, the error E of the reconstructions is normalized by E_0. It can be clearly seen that $\delta = 1$ is associated with the minimal E among all δ considered. This clearly indicates the optimality of our choice of δ.

Table 1 – Comparison of the CPU hours for different reconstruction methods including the standard Y–T stochastic reconstruction using S_2 alone without dilation–erosion, the standard reconstruction using both S_2 and C_2, as well as the dilation–erosion (DE) reconstruction. The simulations were carried out on a standard Dell T5600 workstation.

	S_2 alone reconstruction	S_2–C_2 reconstruction	DE reconstruction
CPU hours	1.6	29.5	1.8

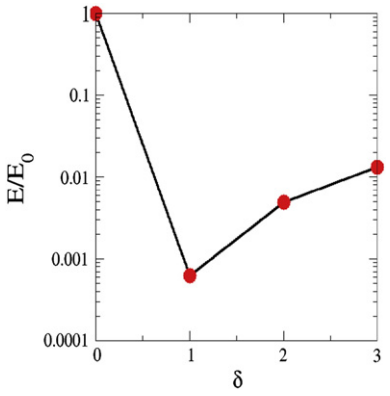

Fig. 8 – Effect of the dilation thickness δ on the accuracy of the dilation–erosion reconstructions.

The dilation–erosion method provides a computationally efficient means for modeling and reconstructing realistic 3D microstructure of topological complex materials from limited morphological information for subsequent analysis of their effective properties and performance. This technique is readily applied to characterize and model other complex filamentary structures such as composites and alloys with microcracks. However, for materials composed of compact well-isolated phases such as particle reinforced composites, directly incorporating the cluster function C_2 into the reconstruction has been shown to be a superior method to accurately characterize and model such structures [36].

Acknowledgments

This work was supported by the Division of Materials Research at National Science Foundation under award No. DMR-1305119. E. G. and T. J. thank the financial support from the National Science and Technology Major Project of the Ministry of Science and Technology of China, under Project Nos. 2011ZX04014-052 and 2012ZX04012011. E. G. is also grateful to the Chinese Scholarship Council for financial support during his stay at Arizona State University (USA) and to the Doctoral Fund of Ministry of Education of China, under Grant No. 20130002110012.

REFERENCES

[1] Torquato S. Microstructure characterization and bulk properties of disordered two-phase media. J Stat Phys 1986;45:843–73.

[2] Torquato S. Random heterogeneous materials: microstructure and macroscopic properties. New York: Springer; 2002.
[3] Sahimi M. Heterogeneous materials I: Linear transport and optical properties. New York: Springer; 2003.
[4] Kak AC, Slaney M. Principles of computerized tomographic imaging. New York: IEEE Press; 1988.
[5] Brandon D, Kaplan WD. Microstructural characterization of materials. New York: John Wiley & Sons; 1999.
[6] Herman RT. Fundamentals of computerized tomography: image reconstruction from projection. 2nd ed. New York: Springer; 2009.
[7] Baruchel J, Bleuet P, Bravin A, Coan P, Lima E, Madsen A, et al. Advance in synchrotron hard X-ray based imaging. C R Physique 2008;9:624–41.
[8] Kinney JH, Nichols MC. X-ray tomographic microscopy (XTM) using synchrotron radiation. Annu Rev Mater Sci 1992;22:121–52.
[9] Padilla E, Jakkali V, Jiang L, Chawla N. Quantifying the effect of porosity on the evolution of deformation and damage in Sn-based solder joints by x-ray microtomography and microstructure-based finite element modeling. Acta Mater 2012;60:4017–26.
[10] Chawla N, Williams JJ, Deng X, McClimon C. Three dimensional (3D) characterization and modeling of porosity in powder metallurgy (P/M) steels. Int J Powder Metall 2009;45:19–27.
[11] Babout L, Maire E, Buffière JY, Fougères R. Characterization by X-ray computed tomography of decohesion, porosity growth and coalescence in model metal matrix composite. Acta Mater 2001;49:2055–63.
[12] Borbély A, Csikor FF, Zabler S, Cloetens P, Biermann H. Three-dimensional characterization of the microstructure of a metal-matrix composite by holotomography. Mater Sci Eng 2004;A367:40–50.
[13] Kenesei P, Biermann H, Borbély A. Structure–property relationship in particle reinforced metal-matrix composites based on holotomography. Scripta Mater 2005;53:787–91.
[14] Williams JJ, Flom Z, Amell AA, Chawla N, Xiao X, De Carlo F. Damage evolution in SiC particle reinforced Al alloy matrix composites by x-ray synchrotron tomography. Acta Mater 2010;58:6194–205.
[15] Silva FA, Williams JJ, Mueller BR, Hentschel MP, Portella PD, Chawla N. 3D microstructure visualization of inclusions and porosity in SiC particle reinforced Al matrix composites by x-ray synchrotron tomography. Metall Mater Trans 2010;A41:2121–8.
[16] Weck A, Wilkinson DS, Maire E, Toda H. Visualization by x-ray tomography of void growth and coalescence leading to fracture in model materials. Acta Mater 2008;56:2919–28.
[17] Toda H, Yamamoto S, Kobayashi M, Uesugi K, Zhang H. Direct measurement procedure for three-dimensional local crack driving force using synchrotron X-ray microtomography. Acta Mater 2008;56:6027–39.
[18] Wang MY, Williams JJ, Jiang L, De Carlo F, Jing T, Chawla N. Three dimensional (3D) experimental characterization by x-ray synchrotron tomography and phase-field simulations. Scripta Mater 2011;65:855–8.
[19] Wang MY, Williams JJ, Jiang L, De Carlo F, Jing T, Chawla N. Three dimensional (3D) microstructural characterization and quantitative analysis of solidified microstructures in magnesium alloys by x-ray synchrotron tomography. Metallogr Microstruct Anal 2012;1:7–13.
[20] Williams JJ, Yazzie KE, Phillips NC, Chawla N, Xiao X, De Carlo F. On the correlation between fatigue striation spacing and crack growth rate: a 3D x-ray synchrotron tomography study. Metall Mater Trans 2011;A42:3845–8.
[21] Torquato S. Random heterogeneous media: microstructure and improved bounds on the effective properties. Appl Mech Rev 1991;44:37–76.
[22] Torquato S. Exact expression for the effective elastic tensor of disordered composites. Phys Rev Lett 1997;79:681–4.
[23] Pham DC, Torquato S. Strong-contrast expansions and approximations for the effective conductivity of multiphase composites. J Appl Phys 2003;94:6591–602.
[24] Lu B, Torquato S. Lineal path function for random heterogeneous materials. Phys Rev 1993;A45:922–9.
[25] Torquato S, Avellaneda M. Diffusion and reaction in heterogeneous media: pore size distribution, relaxation times, and mean survival time. J Chem Phys 1991;95:6477–89.
[26] Torquato S, Beasley JD, Chiew YC. Two-point cluster function for continuum percolation. J Chem Phys 1988;88:6540–7.
[27] Torquato S. Interfacial surface statistics arising in diffusion and flow problems in porous media. J Chem Phys 1986;85:4622–8.
[28] Roberts AP. Statistical reconstruction of three-dimensional porous media from two- dimensional images. Phys Rev 1997; E56:3203–12.
[29] Yeong CLY, Torquato S. Reconstructing random media. Phys Rev 1998;E57:495–506.
[30] Yeong CLY, Torquato S. Reconstructing random media II. Three-dimensional media from two-dimensional cuts. Phys Rev 1998;E58:224–33.
[31] Fullwood DT, Niezgoda SR, Kalidindi SR. Microstructure reconstructions from 2-point statistics using phase-recovery algorithms. Acta Mater 2008;56:942–8.
[32] Hajizadeh A, Safekordi A, Farhadpour FA. A multiple-point statistics algorithm for 3D pore space reconstruction from 2D images. Adv Water Resour 2011;34:1256–67.
[33] Tahmasebi P, Sahimi M. Cross-correlation function for accurate reconstruction of heterogeneous media. Phys Rev Lett 2013;110:078002.
[34] Sheehan N, Torquato S. Generating microstructures with specified correlation functions. J Appl Phys 2001;89:53–60.
[35] Rozman MG, Utz U. Uniqueness of reconstruction of multiphase morphologies from two-point correlation functions. Phys Rev lett 2002;89(13):135501.
[36] Jiao Y, Stillinger FH, Torquato S. A superior descriptor of random textures and its predictive capacity. Proceedings of the National Academy of Sciences of the United States of America; 2009. p. 17634–9 106.
[37] Jiao Y, Stillinger FH, Torquato S. Modeling heterogeneous materials via two-point correlation functions: basic principles. Phys Rev 2007;E76:031110.
[38] Jiao Y, Stillinger FH, Torquato S. Modeling heterogeneous materials via two-point correlation functions: II. Algorithmic details and applications. Phys Rev 2008; E77:031135.
[39] Jiao Y, Pallia E, Chawla N. Modeling and predicting microstructure evolution in lead/tin alloy via correlation functions and stochastic material reconstruction. Acta Mater 2013;61:3370–7.
[40] Singh S, Williams JJ, Jiao Y, Chawla N. Modeling anisotropic multiphase heterogeneous materials via direction correlation functions: simulations and experimental verification. Metall Mater Trans 2012;A43:4470–4.
[41] Zachary CE, Torquato S. Improved reconstructions of random media using dilation and erosion processes. Phys Rev 2011; E84:056102.
[42] Frary ME, Schuh CA. Correlation-space description of the percolation transition in composite microstructures. Phys Rev E 2007;76:041108.
[43] Wilding SE, Fullwood DT. Clustering metrics for two-phase composites. Comput Mater Sci 2011;50:2262–72.
[44] Basinger J, Homer ER, Fullwood DT, Adams BL. Susceptible grain boundary percolation 304 stainless steel. Scrip Mat 2005;53:959.
[45] Gueguen Y, Dienes J. Transport properties of rocks from statistics and percolation. Math Geol 1989;21:1–13.
[46] Fullwood DT, Kalidindi SR, Niezgoda SR, Fast A, Hampson N. Gradient-based microstructure reconstructions from

distributions using fast Fourier transforms. Mater Sci Eng A 2008;494:68–72.
[47] Kirkpatrick S, Gelatt CD, Vecchi MP. Optimization by simulated annealing. Science 1983;220:671–80.
[48] Jiao Y, Stillinger FH, Torquato S. Geometrical ambiguity of pair statistics. II. Heterogeneous media. Phys Rev 2010;E82:011106.
[49] Gommes CJ, Jiao Y, Torquato S. Density of states for a specified correlation function and the energy landscape. Phys Rev Lett 2012;108:080601.
[50] Guo E-Y, Wang M-Y, Jing T, Chawla N. Temperature-dependent mechanical properties of an austenitic–ferritic stainless steel studied by in situ tensile loading in a scanning electron microscope (SEM). Mater Sci Eng 2013; A580:159–68.
[51] Chawla N, Ganesh VV, Wunsch B. Three-dimensional (3D) microstructure visualization and finite element modeling of the mechanical behavior of SiC particle reinforced aluminum composites. Scripta Mater 2004;51:161–5.